ELSEVIER

Journal of Photochemistry and Photobiology A: Chemistry 91 (1995) 7–12

Journal of PHOTOCHEMISTRY AND PHOTOBIOLOGY A: CHEMISTRY

Determination of the free ion yield in photoinduced electron transfer processes using transient thermal phase grating spectroscopy

Arthur Henseler, Eric Vauthey *

Institute of Physical Chemistry of the University of Fribourg, Pérolles, CH-1700 Fribourg, Switzerland

Received 1 March 1995; accepted 9 May 1995

Abstract

An application of transient thermal phase grating spectroscopy with near-infrared probing to the determination of free ion yield in photoinduced electron transfer reactions is presented. The model system is 9,10-dicyanoanthracene with various electron donors in acetonitrile. The measured yields are in good agreement with those obtained from photoconductivity, when the latter are correctly calibrated. The method is explained and its advantages and limitations are discussed.

Keywords: Photothermal spectroscopy; Energetics of electron transfer; Triplet yield; Non-radiative transitions

1. Introduction

The quantum yield of free ion formation ϕ_{ion} is an important parameter in photoinduced intermolecular electron transfer (ET) reactions. From its value, it is, for example, possible to deduce the relative magnitude of the rate of separation of a geminate ion pair into free ions and the rate of back ET within the ion pair. This procedure has allowed the first observation of the Marcus inverted region for intermolecular ET reactions in solution [1,2].

Flash photolysis is the most used technique to measure ϕ_{ion} but requires the knowledge of the extinction coefficient of one of the radical ions. Moreover, in flash photolysis it is very difficult to distinguish absorption of the solvated free ions from that of the geminate ion pair. Finally, some radical ions have very small extinction coefficients, making their observation by absorption problematic. Gould et al. have circumvented the latter problem by using a secondary donor, such as tritolylamine, whose radical cation shows an intense absorption band in the visible region [3]. However, this procedure may lead to erroneous ϕ_{ion} values when the concentration of the primary ions becomes equal to that of the secondary donor. In this case, the homogenous recombination of the ions competes efficiently with the ET between the donor cation and the secondary donor and leads to a too small value of ϕ_{ion} [4]. These various problems do not arise with photoconductivity [4,5]. The intensity of the signal depends on the concentration of the free ions only, and the determination of ϕ_{ion} does not require the knowledge of extinction coefficients. However, to obtain absolute ion yields, the photoconductivity intensity has to be calibrated. It can be calibrated using the method of Ballard and Mauzerall, which requires the knowledge of the equivalent conductance of the ionic species [5]. Another procedure uses as standard the intensity of the photoconductivity signal obtained with a pair of donor/acceptor molecules, having similar shapes and volumes, and with a precisely known value of ϕ_{ion} [4]. However with this calibration method, the performance of photoconductivity relies on the efficiency of a technique allowing absolute ϕ_{ion} to be determined.

In this paper, we present the application of a photothermal method, transient thermal phase grating (TTPG) spectroscopy, for the determination of ϕ_{ion}. Another photothermal method, photoacoustic spectroscopy, has already been used for such measurements [6]. The major drawback of this technique is the relative complexity of the signal analysis, which requires deconvolution of the response function and a fit to a kinetic model. As will be shown here, the extraction of the value of ϕ_{ion} from the TTPG signal is straightforward and does not require any fitting or deconvolution procedure, compensating for the complexity of the experimental set-up. However, the extraction of kinetic parameters from the TTPG signal does require more mathematical effort as in photoacoustic spectroscopy. The reason for probing with a near-infrared (NIR) wavelength (1064 nm) instead of a visible one is to avoid interference with population gratings. Indeed,

* Corresponding author.

SSDI 1010-6030(95)04111-7

many radical ions exhibit a strong absorption in the visible, while they are often transparent in the NIR [7]. The ion yields in the ET reactions between 9,10-dicyanoanthracene and various donors have been determined by TTPG with NIR probing and compared with values obtained with photoconductivity [2,4,8].

2. Principles of TTPG spectroscopy

The theory related to TTPG spectroscopy has been reviewed by several authors [9–12] and therefore only its most significant aspects will be described here. In a transient grating experiment, the sample is excited by two spatially crossed and time-coincident laser pulses producing an interference pattern. This spatially modulated excitation creates in the sample spatial distributions of ground state, excited state and/or photochemical intermediates and product populations. Consequently, similar modulations of the refractive index and absorbance are generated. If non-radiative transitions or exothermic processes take place after excitation, heat is deposited in the medium. This produces a local change of temperature, which generates changes of density and, thereby, of refractive index. Thermoinduced changes of the absorbance can also take place, but in most cases their magnitude is much smaller and can therefore be neglected. The amplitude of these grating-like distributions can be measured by a third, time-delayed laser pulse striking the grating at Bragg angle. If the probing wavelength, λ, does not correspond to the absorption or the refraction spectrum of any species involved in the reaction, the relationship between the diffracted intensity and the amplitude of the thermoinduced refractive index grating or the thermal phase grating, n_1, can be calculated with the following equation proposed by Kogelnik for a plane-wave hologram [13]:

$$\eta = \frac{I_{dif}}{I_{inc}} = \sin^2\left(\frac{\pi n_1 d}{\lambda \cos\theta}\right) \cong \left(\frac{\pi n_1 d}{\lambda \cos\theta}\right)^2 \quad (1)$$

where η is the diffraction efficiency, I_{dif} and I_{inc} are the diffracted and incident light intensities respectively, d is the optical path length and θ is the Bragg angle. The simplification on the r.h.s. of this equation holds for small diffraction efficiencies only, i.e. $\eta \leqslant 0.01$, as is usually the case in TTPG spectroscopy. The time dependence of the modulation amplitude of the thermal phase grating has been described as [10]:

$$n_1(t) = CQ\left[\frac{k_{td}\omega^{-1}\sin(\omega t)e^{-at} - \cos(\omega t)e^{-at} + e^{-k_{td}t}}{k_{td}^2 + \omega^2} - \frac{k_r\omega^{-1}\sin(\omega t)e^{-at} - \cos(\omega t)e^{-at} + e^{-k_r t}}{k_r^2 + \omega^2}\right] \quad (2)$$

where C is a constant that depends on thermal and acoustic properties of the solution, Q is the amount of heat released, a is equal to αv_s, α being the acoustic attenuation and v_s the speed of sound, and ω is the acoustic frequency defined as:

$$\omega = kv_s = \frac{2\pi}{\Lambda} v_s = \frac{4\pi \sin\phi}{\lambda_{exc}} v_s \quad (3)$$

where k is the grating wave vector, Λ the fringe spacing of the grating, and ϕ the angle of incidence of the excitation beams of wavelength λ_{exc}.

The second term in the square brackets of Eq. (2) describes the formation of the thermal phase grating owing to a heat-releasing process with a rate constant k_r and the first term its disappearance by thermal diffusion with a rate constant k_{td}. An important parameter for the time profile of the diffracted intensity owing to a thermal phase grating is the acoustic period, $\tau_{ac} = 2\pi/\omega$. When heat is released within a time shorter than τ_{ac}, the signal is completely modulated by the acoustic response: two counter propagating acoustic waves are generated and the density at the grating peaks oscillates between normal and a reduced value while the density at the grating nulls oscillations between normal and an increased value. On the other hand, when $k_r^{-1} > \tau_{ac}$, the acoustic response is no longer driven impulsively and the dynamics of heat deposition can be resolved.

In what follows, the heat releases will be classified into two groups: fast heat deposition with $k_r^{-1} < \tau_{ac}$, and slow heat deposition with $k_r^{-1} > \tau_{ac}$. If several heat releasing processes take place, the observed diffracted intensity is proportional to the square of the total phase grating amplitude and the maximum diffracted intensity, I_{max}, is proportional to the square of the total amount of heat released, Q_{tot}:

$$I_{dif}(t) \propto \left(\sum_i n_{1,i}(t)\right)^2 \quad I_{max} \propto Q_{tot}^2 = (Q_{fast} + Q_{slow})^2 \quad (4)$$

3. Experimental

3.1. Apparatus

The transient grating set up is depicted in Fig. 1. The third harmonic output at 355 nm of an active/passive mode-locked

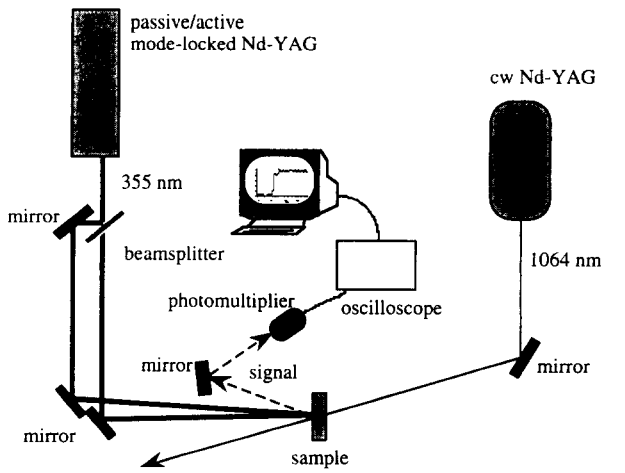

Fig. 1. Schematic representation of the transient thermal phase grating set-up.

Nd:YAG laser (Continuum, model PY61-10) with a pulsewidth of 30 ps is split into two parts which, after travelling an equal amount of distance, are overlapped both in space and time in the sample cell. The total pump intensity on the sample was around 1 mJ cm^{-2}. The resulting transient phase grating is probed at 1064 nm by the 3 W output of a cw-Nd:YAG laser (Quantronix, model 114). The diffracted beam is detected using a NIR-sensitive photomultiplier tube (Hamamatsu, model R406) connected to a 100 MHz oscilloscope (Gould, model 4074), interfaced with a PC. The time resolution of the experiment was about 10 ns, the resolution of the oscilloscope. The signal was averaged over 128 laser shots. Each measurement was repeated three times and the average values were used.

3.2. Samples

9,10-Dicyanoanthracene (DCA) (Kodak), durene and biphenyl (BIP) were sublimed twice under vacuum; benzophenone (BP) (Aldrich) was recrystallised from aqueous ethanol and sublimed twice under vacuum; *N,N*-dimethylaniline and m-xylene were distilled twice. Acetonitrile (MeCN) (Fluka) was of spectroscopic grade and was used as such.

The absorbance of the sample solutions at 355 nm was 0.3 on 1 mm, the cell thickness. All measurements were performed at 20 ± 1 °C.

4. Results and discussion

4.1. Test measurements with known systems

In order to test the performance of the set-up, a few measurements with known systems have been carried out. Fig. 2 shows the time profile of the diffracted intensity observed after excitation of a solution of 2-hydroxybenzophenone (HBP) in methanol. The heat release is due to the very fast relaxation of HBP* to the ground-state by reversible intramolecular proton transfer. As the angle of incidence ϕ is 0.27°, τ_{ac} is of the order of 30 ns. Therefore, the signal is modulated by an acoustic wave, which is attenuated on the microsecond timescale to a constant value that should be

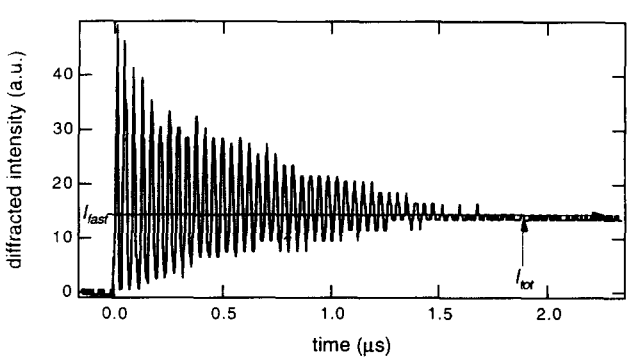

Fig. 2. Time profile of the diffracted intensity measured with a solution of 2-hydroxybenzophenone in methanol with an angle of incidence, ϕ, of 0.27°.

equal to about one quarter of the first peak intensity as expected for the square of a damped oscillation. Owing to the response time of the oscilloscope and to a slight aliasing, the intensity of the initial peak is smaller than four times the value after attenuation. This effect occurs especially when a large amount of fast heat is released. Therefore, the intensity owing to the fast heat release I_{fast} ($I_{fast} \propto Q_{fast}^2$), is obtained by extrapolating the d.c. component of the time profile to time zero. In Fig. 1, Q_{fast} is equal to the total heat release Q_{tot}.

The effect of oxygen on the triplet state of benzophenone (BP) in MeCN is depicted in Fig. 3. The oscillation is due to the fast heat released upon formation of ^{3}BP*, while the rising d.c. component is caused by the slow heat released during the relaxation of ^{3}BP*. As expected for a triplet state, the rate constant of the slow heat release increases substantially with the oxygen content of the solution. In O_2-saturated solution (Fig. 3(a)), the rate constant is so large, that the acoustic amplitude becomes substantially larger. When seen on a longer time scale (Fig. 3(e)), the time profile decays exponentially with a rate constant k_{td} which amounts to 4.7×10^3 s^{-1} with an angle of incidence of 0.27°. The maximum intensity I_{max} (see Eq. (4)), can be obtained by extrapolating this decay to time zero. At short time, the diffracted intensity is due to the fast heat release only, and I_{fast} can in principle be obtained by extrapolating the d.c. component to time zero. In the present case this procedure results in a value for I_{fast} of about zero. However, as the amplitude of the oscillation is small enough to be correctly recorded by the oscilloscope, I_{fast} can be taken as a quarter of the first oscillation maximum and I_{slow} is obtained by considering that $I_{slow}^{1/2} = I_{max}^{1/2} - I_{fast}^{1/2}$. Knowing that for BP all the absorbed energy is transformed into heat $Q_{slow} = (I_{slow}^{1/2}/I_{max}^{1/2}) \times 3.49$ eV, and that the triplet state energy, E_T amounts to 3.0 eV [14], the triplet yield is equal to:

$$\Phi_T = \frac{Q_{slow}}{E_T} \quad (5)$$

From the time profiles shown in Figs. 3(c)–3(e), the triplet yield of BP in MeCN amounts to 0.97 ± 0.05, in agreement with the value reported in the literature [14]. When calculated with the time profile measured with the O_2-saturated solution, a Φ_T value of 0.89 ± 0.05 is obtained. This lower value is owing to the fact that the rate constant of the slow heat release is approaching the limit between slow and fast heat release given by τ_{ac}^{-1}.

This limit can be shifted to faster rates by increasing the angle of incidence of the pump beams. The time profile obtained with BP in MeCN using an angle of incidence, ϕ, of 2.4° is shown in Fig. 3(f). From this trace, a Φ_T value of 0.96 ± 0.05 is obtained. With $\phi = 2.4°$, τ_{ac} amounts to about 3.3 ns and the oscillation cannot be resolved. Moreover, the attenuation constant α depends on the grating wave vector as $\alpha = \text{constant} \times k^2$ and must therefore be more than 75 times larger than with $\phi = 0.27°$ ($\alpha \approx 500$ m^{-1}, $v_s = 1300$ m s^{-1}). However, the rate constant for thermal diffusion k_{td} is also

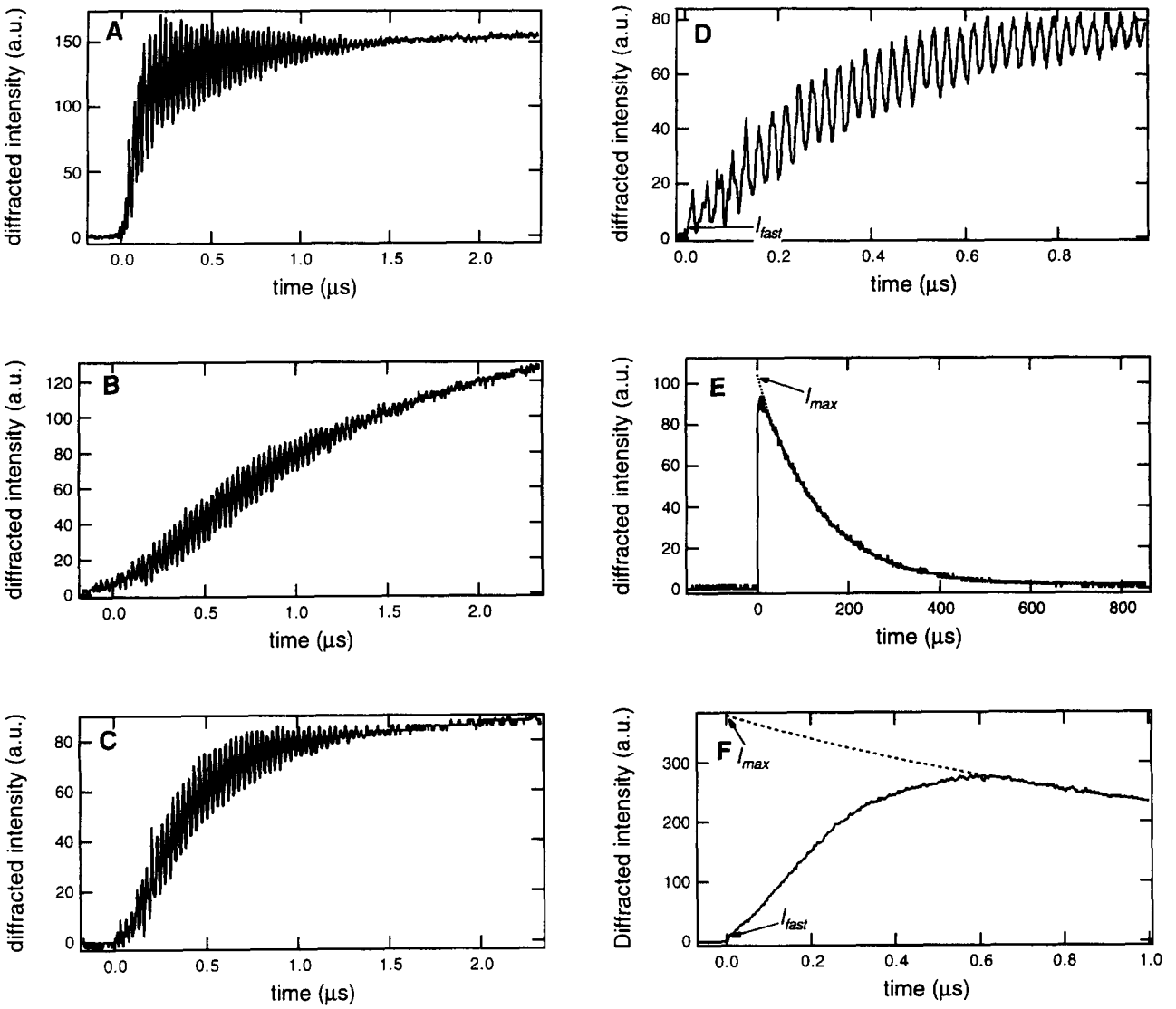

Fig. 3. Time profile of the diffracted intensity measured with a solution of benzophenone in MeCN: (a) O_2-saturated solution; (b) N_2-saturated solution; (c)–(e) aerated solution with $\phi = 0.27°$; and (f) $\phi = 2.4°$.

proportional to k^2 and therefore the decay of the diffracted intensity is much faster than with the small angle, i.e. $k_{td} = 4.7 \times 10^3\ s^{-1}$ with $\phi = 0.27°$ and $k_{td} = 4.5 \times 10^5\ s^{-1}$ with $\phi = 2.4°$. With a large angle of incidence, the diffracted intensity owing to the slow heat release is truncated by the thermal diffusion, making the determination of I_{max} more difficult than with the small angle, especially for heat releases with a time constant of several milliseconds. Hence, a compromise between resolution, acoustic attenuation and thermal diffusion must be found by using the appropriate angle of incidence of the two pump beams.

If the timescales of the heat deposition processes are not different enough from each other, the time profile must be fitted to Eq. (1) in order to determine the different thermalisation parameters.

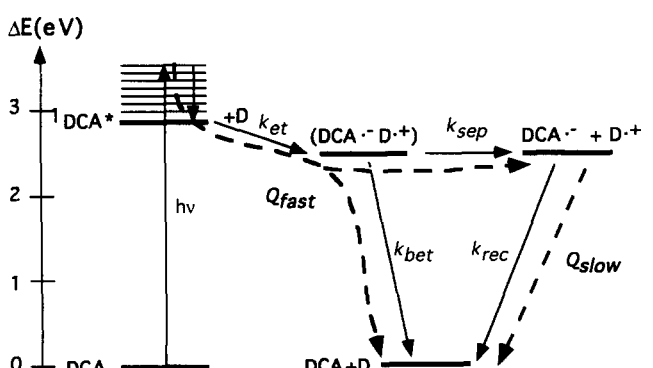

Fig. 4. Energy diagram of the states involved in the photoinduced ET between DCA and various donors in MeCN.

4.2. Measurements of free ion yields

Fig. 4 shows an energy diagram of the states involved in a photoinduced ET between DCA* and various donors in MeCN. After excitation at 355 nm ($E = 3.49$ eV), and vibrational relaxation to the S_1 state ($E_{S1} = 2.96$ eV [15]), DCA* is quenched within about 1 ns by ET with an electron donor

([D] = 0.3 M) and a geminate ion pair is generated. This ion pair can either dissociate with a rate constant k_{sep} of about 5×10^8 s^{-1} into solvated free ions [16] or recombine by back-ET to the neutral ground state. Finally, the free ions decay to the neutral ground state by homogenous recombination in several milliseconds. The free ions yield, Φ_{ion}, is defined as:

$$\Phi_{ion} = \Phi_{gip}\Phi_{sep} = \Phi_{gip}\frac{k_{sep}}{k_{sep} + k_{bET}} \quad (6)$$

where Φ_{gip} is the yield of geminate ion pair formation, Φ_{sep} is the separation efficiency of the geminate ion pair and depends on the relative magnitudes of the rate constants of separation, k_{sep}, and of back-ET, k_{bET}.

As shown in Fig. 4, fast heat is released upon formation of the solvated free ions and back-ET. On the other hand, slow heat is generated by the homogenous recombination of the free ions. With the concentration of donor used, $\Phi_{gip} = 1$ (except for BIP, vide infra) and consequently:

$$\Phi_{ion} = \Phi_{sep} = \frac{Q_{slow}}{\Delta H_{fi}} \quad (7)$$

where ΔH_{fi} is the enthalpy of formation of the free ions from the neutrals in the ground state and is given by [17]:

$$\Delta H_{fi} = E_{ox}(D) - E_{red}(A) + T\Delta S_{fi} \quad (8)$$

where $E_{red}(A)$ and $E_{ox}(D)$ are the reduction and oxidation potentials of the acceptor ($E_{red}(DCA) = -0.89$ V vs. SCE [15]) and donor (see Table 1) respectively and ΔS_{fi} is the entropy difference between the free ions and the neutrals. This change of entropy is mainly due to the loss of degrees of freedom of the polar solvent molecules around the free ions and has been estimated as $\Delta S_{fi} = 0.08$ eV in MeCN [12].

Fig. 5 shows a time profile obtained with a solution of DCA and 0.3 M BIP in MeCN. From the values of I_{max} and I_{fast}, and using $\Delta H_{fi} = 2.97$ eV, Φ_{ion} amounts to 0.48 ± 0.03. The rate constant for quenching of DCA* by BIP amounts to 3.06×10^9 M^{-1} s^{-1} [18] and is substantially smaller than the diffusion limit in MeCN ($k_{diff} \approx 2 \times 10^{10}$ M^{-1} s^{-1}), Φ_{gip} amounts to 0.95 with [BIP] = 0.3 M and $\Phi_{sep} = 0.50 \pm 0.3$. The separation efficiencies with four other donors are listed in Table 1 together with values obtained from photoconductivity measurements [2,4,8]. It can be seen that the values

Table 1
Separation efficiencies of DCA with different electron donors in MeCN obtained from TTPG spectroscopy (third column, limit of error ±0.03), from photoconductivity assuming an ion yield for BP/DABCO of 0.85 (fourth column) and of unity (fifth column)

Donor	E_{ox} (V vs. SCE)	Φ_{sep} (TTPG)	Φ_{sep}	Φ_{sep} (cor)
biphenyl	1.91 [22]	0.50	0.41	0.49
p-xylene	1.86 [23]	0.36	0.33	0.39
durene	1.62 [22]	0.20	0.16	0.19
N,N-dimethylaniline	0.79 [24]	≈0	0.01	0.02
t-silbene	1.45 [25]	0.16	0.12	0.14

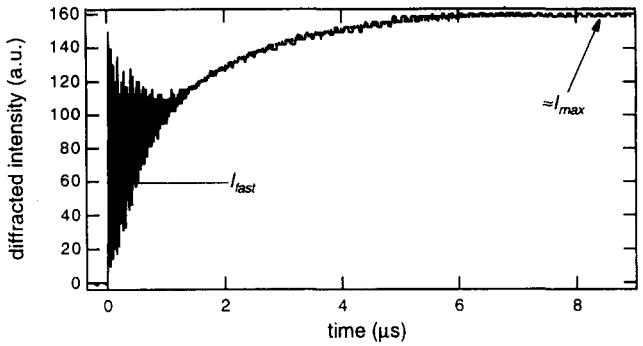

Fig. 5. Time profile of the diffracted intensity measured with a solution of DCA with 0.3 M biphenyl in MeCN. I_{fast} and I_{max} are obtained by extrapolating the rising d.c. component and the decay of the diffracted intensity (not shown) to time zero, respectively.

obtained from the TTPG measurements are systematically about 18% larger that those obtained from photoconductivity. For those measurements, the standard system was BP/DABCO (1,4-diazabicyclooctane) in MeCN, with a Φ_{ion} value of 0.85 taken from the literature [19,20]. The ion yield for this system has been measured by TTPG spectroscopy and a value close to unity has been obtained [21]. Table 1 shows that when corrected to a BP/DABCO ion yield of unity, the yields obtained from photoconductivity are in excellent agreement with those measured by TTPG spectroscopy.

5. Conclusion

The present results show that TTPG spectroscopy is a valuable technique for determining absolute free ion yields. However, owing to the quadratic dependence of the signal on the energy release and to the uncertainty in the values of ΔH_{fi}, this technique is not reliable for free ion yields smaller than 0.05. For such small yields, photoconductivity has to be used, but the signal intensity has to be correctly calibrated. The greatest advantages of TTPG spectroscopy over the other photothermal methods are the time resolution, the relatively easy extraction of the thermalisation parameters from the observed signal, and the possibility to shift the limit between fast and slow heat releases by varying the angle of incidence of the pump beams.

Acknowledgements

We wish to thank Professor P. Suppan for helpful advice and discussions. We also express our thanks to Professor E. Haselbach for his continuing support and encouragement. This work was supported by the Fonds National Suisse de la Recherche Scientifique through project number 21-36150.92 and by the programme d'encouragement à la Relève Universitaire de la Confédération.

References

[1] I.R. Gould, D. Ege, S.L. Mattes and S. Farid, *J. Am. Chem. Soc., 109* (1987) 3794.

[2] E. Vauthey, P. Suppan and E. Haselbach, *Helv. Chim. Acta, 71* (1988) 93.

[3] I.R. Gould, D. Ege, J.E. Moser and S. Farid, *J. Am. Chem. Soc., 112* (1990) 4290.

[4] E. Vauthey, D. Pilloud, E. Haselbach, P. Suppan and P. Jacques, *Chem. Phys. Lett., 215* (1993) 264.

[5] S.G. Ballard and D.C. Mauzerall, *J. Chem. Phys., 72* (1980) 933.

[6] J. Feitelson and D.C. Mauzerall, *J. Phys. Chem., 97* (1993) 8410.

[7] T. Shida, *Electronic Absorption Spectra of Radical Ions*, Elsevier, Amsterdam, 1988.

[8] D. Burget, P. Jacques, E. Vauthey, P. Suppan and E. Haselbach, *J. Chem. Soc. Faraday Trans., 90* (1994) 2481.

[9] K.A. Nelson, R. Casalegno, R.J.D. Miller and M.D. Fayer, *J. Chem. Phys., 77* (1982) 1144.

[10] L. Genberg, Q. Bao, S. Gracewski and R.J.D. Miller, *Chem. Phys., 131* (1989) 81.

[11] M. Terazima and N. Hirota, *J. Chem. Phys., 95* (1991) 6490.

[12] E. Vauthey and A. Henseler, *J. Phys. Chem., 99* (1995) 8652.

[13] H. Kogelnik, *Bell System Technol. J., 48* (1969) 2909.

[14] A. Lamola and G.S. Hammond, *J. Chem. Phys., 43* (1965) 2129.

[15] A. Padwa, in S.L. Mattes and S. Farid (eds.), *Organic Photochemistry*, Vol. 6, M. Dekker, New York, 1983.

[16] K. Schulten, H. Staerk, A. Weller, H.J. Werner and B. Nickel, *Z. Phys. Chem. N.F., 101* (1976) 371.

[17] A. Weller, *Z. Phys. Chem. N.F., 133* (1982) 93.

[18] D. Pilloud, *Ph.D. Thesis*, University of Fribourg, 1993.

[19] E. Haselbach, E. Vauthey and P. Suppan, *Tetrahedron, 44* (1988) 7335.

[20] H. Miyasaka, K. Morita, K. Kamada and N. Mataga, *Chem. Phys. Lett., 178* (1991) 504.

[21] E. Vauthey and A. Henseler, to be published.

[22] L. Eberson and K. Nyberg, *J. Am. Chem. Soc., 88* (1966) 1686.

[23] W.C. Neikam, G.R. Dimeler and M.M. Desmond, *J. Electrochem. Soc., 111* (1964) 1190.

[24] P. Iwa, U.E. Steiner, E. Vogelmann and H.E.A. Kramer, *J. Phys. Chem., 86* (1982) 6143.

[25] T. Kubota, B. Uno, Y. Matsuhisa, H. Miyasaki and K. Kano, *Chem. Pharm. Bull., 31* (1983) 373.